D-π-A Dye System Containing Cyano-Benzoic Acid as Anchoring Group for Dye-Sensitized Solar Cells

Masataka Katono,[†] Takeru Bessho,[†] Sheng Meng,[‡] Robin Humphry-Baker,[†] Guido Rothenberger,[†] Shaik M. Zakeeruddin,[†] Efthimios Kaxiras,[§] and Michael Grätzel*,[†]

[†]Laboratory for Photonics and Interfaces, Institute of Chemical Sciences and Engineering, Swiss Federal Institute of Technology, CH-1015 Lausanne, Switzerland

[‡]Beijing National Laboratory for Condensed Matter Physics, and Institute of Physics, Chinese Academy of Sciences, 100190 Beijing, China

[§]Department of Physics and School of Engineering and Applied Sciences, Harvard University, Cambridge, Massachusetts 02138, United States

ABSTRACT: A D-π-A dye (KM-1) incorporating cyano-benzoic acid as a new acceptor/anchoring group has been synthesized for dye-sensitized solar cells (DSCs) with a high molar extinction coefficient of 66 700 $M^{-1} cm^{-1}$ at 437 nm. Theoretical calculations show that the hydrogen bond between —CN and surface hydroxyl leads to the most stable configuration on the surface of TiO_2. In addition, the adsorption of the dye on TiO_2 follows a Brunauer—Emmett—Teller (BET) isotherm. Multilayer adsorption of KM-1 on TiO_2 seems to take place particularly at higher dye concentrations. DSC device using KM-1 reached a maximum incident photon-to-current conversion efficiency (IPCE) of 84%, with a solar to electric power conversion efficiency (PCE) of 3.3% at AM1.5 G illumination (100 mW cm^{-2}). This new type of anchoring group paves a way to design new dyes that combine good visible light harvesting with strong binding to the metal oxide surface.
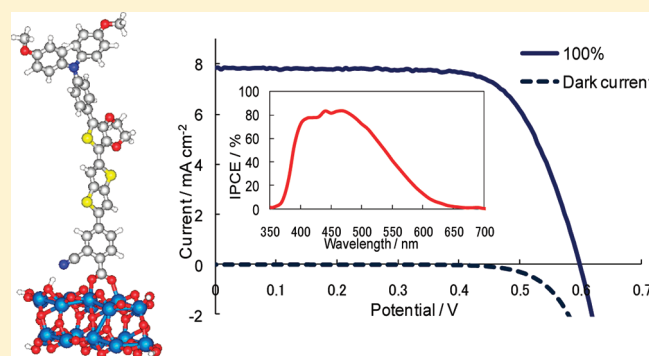
INTRODUCTION

Dye-sensitized solar cells (DSCs) have attracted much attention in recent years due to their potential advantages of low cost, ease of production, flexibility, and transparency relative to conventional crystalline silicon solar cells. The photosensitizer is a key component of the DSC, being responsible for the capture of sunlight and generation of electric charges. State-of-the-art DSCs using ruthenium sensitizers exhibit record solar to electricity power conversion efficiencies (PCEs) of over 11—12% under AM 1.5 G irradiation.[1,2] The performance of DSCs based on metal-free organic sensitizers has also recently been improved, with PCE of up to 10% values having been reported.[3−7] Most efficient metal-free organic sensitizers are D-π-A systems, composed of donor, π-conjugated spacer, and acceptor/anchoring groups. Organic dyes have advantages as photosensitizers due to their high molar extinction coefficients, tuning of absorption wavelength, and relatively facile design and synthesis. Several synthetic strategies for the development of organic sensitizers have been introduced to enhance their performance. These include the incorporation of various functional groups, such as fluorene, coumarin, indoline, cyanine, perylene, triarylamine, and xanthenes, to the donor part.[8,9] A successful approach was to add a π-conjugated linker such as thiophene, thienothiophene, 3,4-ethylenedioxy-thiophene (EDOT), benzo[1,2,5]-thiadiazole, *p*-phenylene vinylene,

and quinoline derivatives for the improvement of efficiency and stability.[8,9] On the contrary, the acceptor/anchoring group has been much less investigated, with cyanoacrylic acid being most widely employed to attach the organic dye to the surface of the titania nanocrystals. In this paper, we report on a novel organic sensitizer, coded KM-1, exhibiting extended π-conjugation at the acceptor/anchoring group. As shown in Figure 1, the KM-1 contains alkoxytriphenylamine as a donor, a binary π-conjugated spacer composed of a thienothiophene, an EDOT unit, and a cyano-benzoic acid as the novel acceptor/anchoring group. This way we created directionality in the molecule to inject excited electron into the TiO_2 conduction band.

EXPERIMENTAL SECTION

Materials. Thienothiophene **1** was prepared as previously reported.[3] All chemicals and solvents were purchased from commercial sources and used without further purification. The methyl 4-chloro-2-cyanobenzoate was obtained from 3B Scientific Corporation.

Synthesis of 4-{7-(5-Bromothieno[3,2-b]thiophen-2-yl)-2,3-dihydrothieno[3,4-b][1,4]dioxin-5-yl}-N,N-bis(4-hexyl-

Figure 1. Molecular structure of the KM-1 dye.

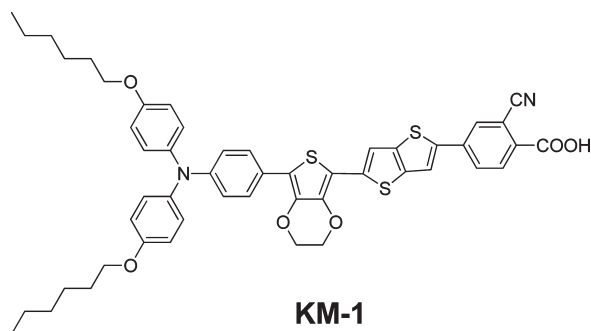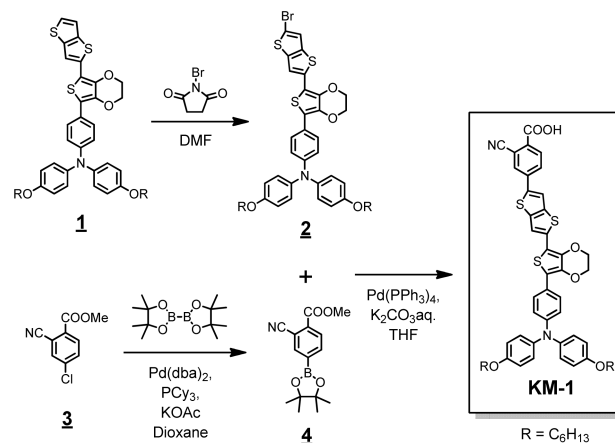**Scheme 1. Synthetic Route of the KM-1 Dye**

oxyphenyl)aniline (2). A solution of **1** (0.543 g, 0.750 mmol) in *N,N′*-dimethylformamide (DMF; 7 mL) at 0 °C was charged with a solution of *N*-bromosuccinimide (0.134 g, 0.750 mmol) in DMF (5 mL). After 3 h stirring at 0 °C, crushed ice was added and the mixture solution was extracted with dichloromethane (3 × 12 mL). The combined organic layers were washed with water (3 × 60 mL) and dried over anhydrous MgSO$_4$. The solvent was removed and the residue was purified on a silica gel column with EtOAc/hexane (1/100, v/v) to obtain **2** in 60% yield (0.358 g). ^{1}HNMR (DMSO-d_6, 400 MHz): δ 0.88 (t, *J* = 7.2 Hz, 6H), 1.31 (m, 8H), 1.41 (m, 4H), 1.71 (m, 4H), 3.93 (t, *J* = 6.4 Hz, 4H), 4.37 (m, 2H), 4.42 (m, 2H), 6.78 (d, *J* = 8.8 Hz, 2H), 6.89 (d, *J* = 8.8 Hz, 4H), 7.01 (d, *J* = 8.8 Hz, 4H), 7.47 (d, *J* = 8.8 Hz, 2H), 7.51 (s, 1H), 7.61 (s, 1H). MS (ESI): *m/z* calcd for C$_{42}$H$_{42}$BrNO$_4$S$_3$: 803.16. Found: 803.16 [M$^+$].

Synthesis of Methyl 2-Cyano-4-(4,4,5,5-tetramethyl-1,3,2-dioxaborolan-2-yl)benzoate (4). A 100 mL flask with a magnetic stirring bar, a septum inlet, and a condenser was charged with Pd(dba)$_2$ (0.17 g, 0.3 mmol) and tricyclohexylphosphine (0.20 g, 0.72 mmol) under nitrogen. Dioxane (35 mL) was added, and the resulting mixture was then stirred for 30 min at room temperature. Bis(pinacolato)-diboron (2.79 g, 11 mmol), KOAc (1.47 g, 15 mmol), and **3** (1.96 g, 10 mmol) were added successively. After being stirred at 80 °C for 19 h, the reaction mixture was treated with water (30 mL). The product was extracted with toluene, washed with brine, and dried over MgSO$_4$. Removal of the solvent followed by trituration with methanol gave **4** as white solid in 45% yield (1.29 g). ^{1}H NMR (CDCl$_3$, 400 MHz): δ 1.36 (s, 12H), 4.00 (s, 3H), 8.05 (d, *J* = 7.6 Hz, 1H), 8.10 (d, *J* = 7.6 Hz, 1H), 8.22 (s, 1H).

Synthesis of 4-{5-{7-{4-{Bis(4-hexyloxyphenyl)amino}-phenyl}-2,3-dihydrothieno[3,4-b][1,4]dioxin-5-yl}thieno-[3,2-b]thiophen-2-yl}-2-cyanobenzoic Acid (KM-1). **2** (0.132 g, 0.164 mmol), **4** (0.0566 g, 0.197 mmol), K$_2$CO$_3$ (0.099 g, 0.716 mmol), and Pd(PPh$_3$)$_4$ (0.024 g, 0.02 mmol) were dispersed in a mixture of tetrahydrofuran (10 mL) and water (2 mL). After the reaction was performed at 80 °C for 68 h, the mixture was diluted with water (20 mL) and CH$_2$Cl$_2$ (30 mL) and then acidified with 1 M HCl under cooling (at 0 °C) condition. The organic layer was separated and subsequently dried over anhydrous MgSO$_4$. The solvent was removed and the residue was purified on a silica gel column with MeOH/CH$_2$Cl$_2$ (1/5, v/v) to obtain KM-1 as brown solid in 50% yield (0.071 g). ^{1}H NMR (DMSO-d_6, 400 MHz): δ 0.88 (t, *J* = 7.2 Hz, 6H), 1.31 (m, 8H), 1.41 (m, 4H), 1.70 (m, 4H), 3.93 (t, *J* = 6.4 Hz, 4H), 4.37 (m, 2H), 4.44 (m, 2H), 6.78 (d, *J* = 8.8 Hz, 2H), 6.89 (d, *J* = 8.8 Hz, 4H), 7.00 (d, *J* = 8.8 Hz, 4H), 7.47 (d, *J* = 8.8 Hz, 2H), 7.55 (s, 1H), 7.83 (d, *J* = 8.0 Hz, 1H), 8.03 (m, 3H). MS (ESI): *m/z* calcd for C$_{50}$H$_{48}$N$_2$O$_6$S$_3$: 868.27. Found: 868.32 [M$^+$].

Differential Pulse Voltammetry (DPV) Measurement. KM-1 in a DMF solution containing tetrabutylammonium hexafluorophosphate (0.1 M) was used as a supporting electrolyte. DPV was measured with glassy carbon as the working electrode and Pt as the counter electrode under Ar atmosphere, and the redox potentials were calibrated with ferrocene as the internal reference.

Cell Fabrication. A state-of-the art double layer mesoporous TiO$_2$ layer (8.2 μm of 20 nm particle; DSL 18NR-T, DYESOL) plus 4.5 μm of 400 nm light scattering particles (HPW-400NRD, CCIC)) was employed on FTO conducting glass (Solar-4 mm, Nippon Sheet Glass Co., Ltd.). The double layer TiO$_2$ film was sensitized by immersing it into a KM-1 solution (0.1 mM) in DMF for 16 h at room temperature. The composition of the electrolyte is 1.0 M 1,3-dimethylimidazolium iodide, 50 mM LiI, 30 mM I$_2$, 0.5 M *tert*-butylpyridine, and 0.1 M guanidinium thiocyanate in a mixture of acetonitrile and valeronitrile (85/15, v/v). A platinized FTO conducting glass (LOF TECH 7, Pilkington) was used as counter electrode. The spectral distribution of the light source simulated the AM 1.5G solar irradiation (Xe 450W/K113 (filter) with a mismatch less than 4%). The device active area is 0.16 cm^2, covered with black tape mask for excluding any diffused light. An antireflection film (ARCTOP, Mihama Co.) was attached on the photoanode side.

Calculations. First-principles calculations were performed within the framework of density functional theory (DFT) for structure optimization and TDDFT for excited states and optical absorption, using SIESTA[10] and Gaussian[11] packages. For structure, we used pseudopotentials of the Troullier-Martins type to model the atomic cores, the PBE form of the exchange-correlation functional, and a local basis set of double-polarized orbitals (19 orbitals for Ti; 13 orbitals for C, N, O and S; 5 orbitals for H). An auxiliary real space grid equivalent to a plane-wave cutoff of 100 Ry was used. A molecular structure was considered fully relaxed when the magnitude of forces on the atoms was smaller than 0.02 eV/Å. Optical absorptions are extracted from TDDFT simulations within linear response theory and using a long-range corrected functional ωB97X.[12] We used the 6-31G(d) basis set. The impact of geometry optimization procedures and basis- sets on atomic structure and excitation energies are shown to be negligible.
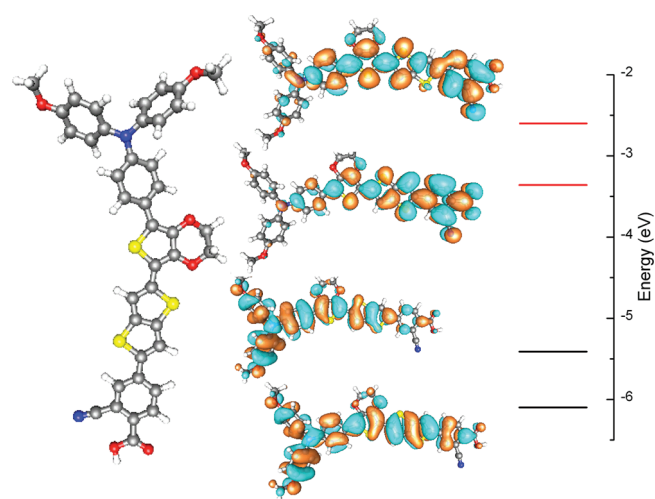
■ RESULTS AND DISCUSSION

The KM-1 dye was synthesized in three steps as shown in Scheme 1. **1** was treated with *N*-bromosuccinimide (NBS) to yield bromothienothiophene **2**. The cyano-benzoic acid anchoring group was synthesized by the palladium-catalyzed Suzuki coupling reaction of **2**, pinacolate **4**, and tetrakis triphenylphosphine palladium to yield finally the KM-1 sensitizer. Synthetic details are given in the Experimental Section.

As shown in Figure 2, the electronic absorption spectrum (CARY 5, Varian) of the KM-1 dissolved in DMF exhibits a strong absorption band at 437 nm and a weaker band appearing
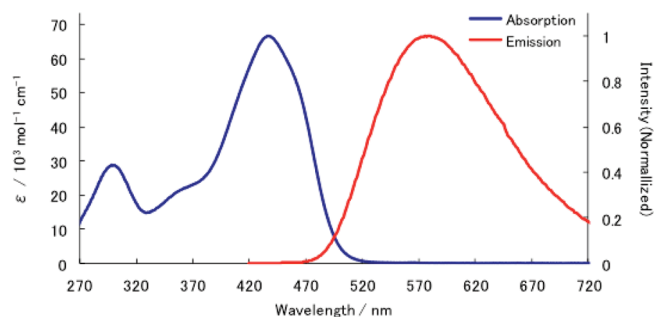
Figure 2. Electronic absorption (blue line) and emission (red line) spectrum of the KM-1 dissolved in DMF.

Table 1. Theoretical Excited-State TD-FDT/ωB97X Calculation of KM-1 Dye, and Comparison with Experiment[a]

n	E (eV, nm)	f	composition	expt
1	2.89 (429)	2.285	43% H→L; 25% H-1→ L	440 nm
2	3.74 (331)	0.121	29% H→ L+1; 24% H-1→ L	350 nm
3	4.30 (288)	0.200	44% H-1→L+1	300 nm

[a] E = calculated absorption energy, f = oscillator's strength, and expt = experimental result. H stands for HOMO, and L for LUMO.

Figure 3. Optimized geometry of model KM-1 dye, corresponding wave functions at the isosurface level of 0.03 e/Å^3 for HOMO-1, HOMO, LUMO, and LUMO+1 orbitals (from bottom to up) and energy levels from DFT/B3LYP. The levels are downshifted by 0.31 eV to match HOMO to the experimental value (−5.41 eV).

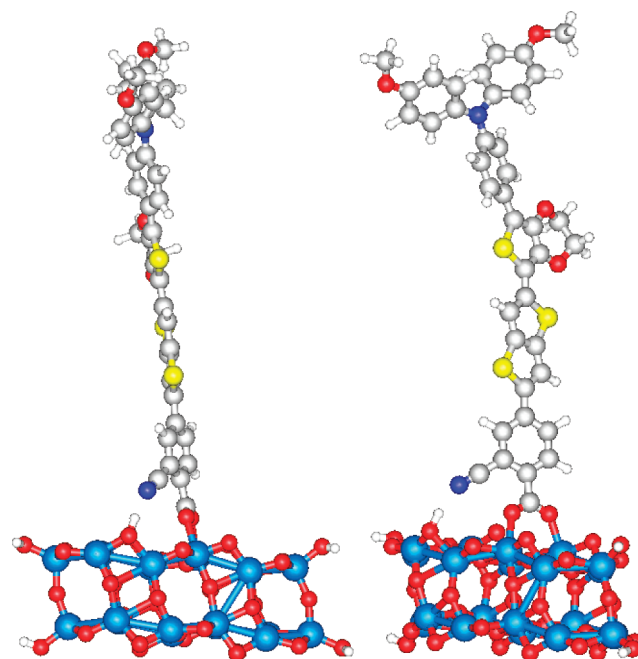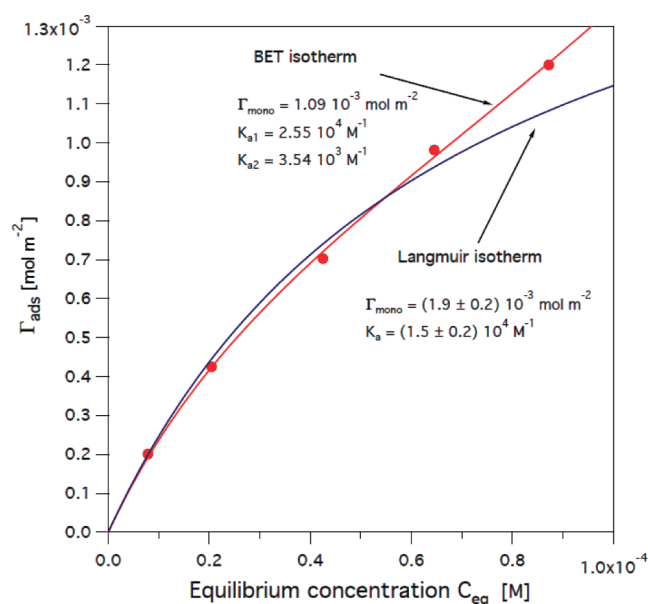**Figure 4.** Side and front views of KM-1 adsorption on a TiO$_2$ nanoparticle.

at 300 nm. The molar extinction coefficients of the peaks at 300 and 437 nm are 28 800 and 66 700 M^{-1} cm^{-1}, respectively. The high molar extinction coefficient of this dye allows us to use thinner TiO$_2$ films as photoanodes in the fabrication of DSCs. The peak absorption of KM-1 on the TiO$_2$ film is shifted by about 10 nm to shorter wavelength compared to that in solution, which may be due to H aggregation of dye on the surface of TiO$_2$. A broadening of the absorption tail to longer wavelength is also observed improving the photoresponse. The emission spectrum was measured using a 480 nm excitation wavelength and was photometrically corrected (Fluorolog 3, HORIBA).

DPV was used to determine the redox potentials of the KM-1 dye. Reversible oxidation and reduction waves were observed at 0.31 V and −2.14 V (vs Fc$^+$/Fc), respectively. The energy offset of the LUMO (−3.1 eV) of the dye molecule with respect to the titania conduction band edge (−4.0 eV) provides the thermodynamic driving forces for charge separation. In this case, the LUMO and CB offset is 0.9 eV; by reducing this gap, one can red-shift the absorption spectra to absorb more visible light and enhance the photoconversion efficiency. The energy offset of the HOMO (−5.41 eV) is relative to that of the iodide (−4.8 eV). The fact that >80% incident photon-to-current conversion efficiency (IPCE) was obtained with the DSCs employing the KM-1 dye proves that 0.61 eV difference between the HOMO

and the redox potential of the electrolyte is sufficient to regenerate the dye, in keeping with earlier observations.

Figure 3 shows the optimized molecular structure and frontier molecular orbitals of KM-1 (for simplicity, we consider R = CH$_3$). The molecule retains perfect planar geometry, with only −C$_2$H$_4$ in EDOT and the donor tails slightly protruding from the molecular plane. Wave functions are mainly distributed around the donor and the acceptor group for the occupied (HOMO-1 and HOMO) and unoccupied orbitals (LUMO, LUMO+1), respectively, favoring fast electron−hole separation upon photoexcitation. We also compared the energy levels at the B3LYP level to experiment: after an empirical downshift of 0.31 eV, calculated orbital levels match experimental ones nicely; see Figure 3.

To gain more insight into its optical property, we also calculated the absorption spectrum of KM-1 using TDDFT with a long-ranged corrected functional (ωB97X) in DMF solution. The results are summarized in Table 1. Low-energy excitations agree well with experimental data and mainly come from transitions involving HOMO-1, HOMO, LUMO, and LUMO+1 orbitals.

A particular advantage of cyano-benzoic acid as an acceptor in KM-1 dye structure is that it strongly enhances dye binding onto TiO$_2$ surfaces compared to cyano-acrylic acid. We investigated the binding geometries of KM-1 on anatase TiO$_2$ (101) using

Figure 5. Langmuir isotherm curve (blue) and BET isotherm curve (red).

Figure 6. $I-V$ characteristics of a DSC sensitized with KM-1 measured under AM 1.5 G sunlight at 100% sunlight (blue), and incident photon to current conversion efficiency curve (red).

DFT. Among several stable-binding configurations, the one with a bidentate bond and a hydrogen bond between −CN and surface hydroxyl (originating from dissociated carboxylic acid upon adsorption) is the most stable configuration with a binding energy of 1.52 eV (see Figure 4). The bond lengths are $d_{Ti1-O1} =$ 2.146 Å, d_{Ti2-O2} = 2.162 Å, and $d_{CN\cdots HO}$ = 1.80 Å. Since three bonds are formed, which is not possible in cyano-acrylic acid anchoring groups, the KM-1 is strongly stabilized on TiO$_2$.

The adsorption equilibrium of KM-1 on TiO$_2$ was also investigated. Figure 5 shows the surface concentration Γ_{ads} of the adsorbed dye as a function of the equilibrium concentration C_{eq} in the DMF solution. Γ_{ads} is calculated from the amount of dye desorbed from the TiO$_2$ film using a 0.05 M tetrabutylammonium hydroxide solution in DMF and from the projected area of the TiO$_2$ film (0.16 cm^2). The experimental Γ_{ads} versus C_{eq} data was fitted to a Langmuir isotherm (eq 1) and to a Brunauer−Emmett−Teller (BET) isotherm (eq 2).

$$\Gamma_{ads} = \frac{\Gamma_{mono} K_a C_{eq}}{1 + K_a C_{eq}} \qquad (1)$$

$$\Gamma_{ads} = \frac{\Gamma_{mono} K_{a1} C_{eq}}{\left\{1 + (K_{a1} - K_{a2}) C_{eq}\right\}\left(1 - K_{a2} C_{eq}\right)} \qquad (2)$$

Here, Γ_{mono} is the surface concentration of the dye that corresponds to monolayer coverage of the interface. In the Langmuir equation, which assumes that a single layer can cover the surface at most, K_a is the adsorption equilibrium constant. By contrast, the BET model allows for multilayer adsorption. K_{a1} is the equilibrium constant for adsorption of the dye on the solid, and K_{a2} is the equilibrium constant for adsorption on sites that are already occupied by adsorbed dye molecules. The best-fit parameters obtained for these variables are given as insets in Figure 5.

With an estimated roughness factor of 1060 for the TiO$_2$ film, an effective area per KM-1 dye molecule of 90 Å^2 is calculated from the value of Γ_{mono} in the Langmuir isotherm case. The
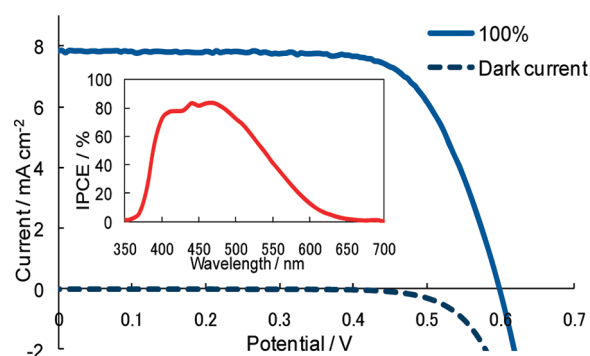
corresponding value obtained in the BET case is 160 Å^2. From molecular modeling, an approximate area of the cross section of the molecule is 110 Å^2 (Figure 4), which is larger than the area predicted from the fitting to the Langmuir isotherm. This observation, together with the fact that the BET isotherm leads to a better fit to the experimental data, particularly at higher concentrations, seems to indicate that multilayer adsorption of KM-1 on TiO$_2$ takes place.

Preliminary photovoltaic tests were conducted to evaluate the potential of KM-1 as a sensitizer in DSC. The photocurrent action spectrum of DSC with the KM-1 as sensitizer is shown in Figure 6 as an inset. The IPCE exceeds 70% from 390 to 510 nm, reaching the maximum of 84% at 470 nm. This high value shows efficient electron injection from the KM-1 excited state to the conduction band of the TiO$_2$ due to sufficiently strong electronic coupling between cyano-benzoic acid and 3d orbitals of TiO$_2$. The broadened and red-shifted IPCE spectrum of the KM-1 in Figure 6, compared to the absorption spectrum of the KM-1 in solution, can be ascribed to the influence of the double layer at the TiO$_2$/electrolyte interface and/or to aggregation of the dye. As shown in Figure 6, the short-circuit photocurrent density (J_{sc}), open-circuit photovoltage (V_{oc}), and fill factor (FF) of DSC at AM1.5G conditions (100 mW cm^{-2}) are 7.8 mA cm^{-2}, 600 mV, and 0.705, respectively, yielding photo conversion efficiency (η) of 3.3%.

■ CONCLUSIONS

In summary, we designed and synthesized a novel high molar extinction coefficient organic sensitizer, KM-1, with cyano-benzoic acid as an acceptor/anchoring group. The theoretical calculations show that the hydrogen bond between −CN and surface hydroxyl is the most stable configuration on the surface of TiO$_2$. The adsorption of the dye follows the BET isotherm. The DSC device with KM-1 reached the maximum IPCE of 84%, with a photoconversion efficiency of 3.3% at AM1.5 G illumination (100 mW cm^{-2}). This shows that cyano-benzoic acid is a potential unit as a new acceptor/anchoring group. We are currently investigating this novel anchoring group linked to high molar extinction dyes that shift the spectral response of the cell to the red region of the solar spectrum, in order to enhance the device performance. In KM-1 dye, the driving force for the electron injection from the excited state of the sensitizer into the TiO$_2$ conduction band is excessive. Hence, there is a room for red-shifting the absorption of the sensitizer by lowering its

LUMO level without sacrificing the yield of injection. The spectral response could be broadened or red-shifted by varying the position of cyano group on the benzoic acid or by substituting the COOH group at the *meta* position of benzene instead of the *para* position.

■ AUTHOR INFORMATION

Corresponding Author
*E-mail: michael.graetzel@epfl.ch. Telephone: +41 (0) 21 693 31 12. Fax: +41 (0) 21 693 61 00.

■ ACKNOWLEDGMENT

■ REFERENCES

(1) Grätzel, M. *Acc. Chem. Res.* **2009**, *42*, 1788−1798.

(2) (a) Chen, C.; Wang, M.; Li, J.; Pootrakulchote, N.; Alibabaei, L.; Ngoc-le, C.; Decoppet, J.; Tsai, J.; Grätzel, C.; Wu, C.; Zakeeruddin, S. M.; Grätzel, M. *ACS Nano* **2009**, *3*, 3103. (b) Gao, F.; Wang, Y.; Shi, D.; Zhang, J.; Wang, M.; Jing, X.; Humphry Baker, R.; Wang, P.; Zakeeruddin, S. M.; Grätzel, M. J. *Am. Chem. Soc.* **2008**, *130*, 10720−10728. (c) Yu, Q.; Wang, Y.; Yi, Z.; Zu, N.; Zhang, J.; Zhang, M.; Wang, P. *ACS Nano* **2010**, *4* (10), 6032. (d) Chiba, Y.; Islam, A.; Watanabe, Y.; Komiya, R.; Koide, N.; Han, L. *Jpn. J. Appl. Phys., Part 2* **2006**, *45*, L638−L640.

(3) Zhang, G.; Bala, H.; Cheng, Y.; Shi, D.; Lv, X.; Yu, Q.; Wang, P. *Chem. Commun.* **2009**, 2198−2200.

(4) Zeng, W.; Cao, Y.; Bai, Y.; Wang, Y.; Shi, Y.; Zhang, M.; Wang, F.; Pan, C.; Wang, P. *Chem. Mater.* **2010**, *22*, 1915−1925.

(5) Ito, S.; Miura, H.; Uchida, S.; Takata, M.; Sumioka, K.; Liska, P.; Comte, P.; Pechy, P.; Grätzel, M. *Chem Commun.* **2008**, 5194.

(6) Li, R.; Liu, J.; Cai, N.; Zhang, M.; Wang, P. J. *Phys. Chem. B* **2010**, *114*, 4461.

(7) Zhu, W.; Wu, Y.; Wang, S.; Li, W.; Li, X.; Chen, J.; Wang, Z.-S.; Tian, H. *Adv. Funct. Mater.* **2011**, *21*, 756.

(8) (a) Mishra, A.; Fischer, M.; Bäuerle, P. *Angew. Chem., Int. Ed.* **2009**, *48*, 2474 and references cited therein. (b) Alibabaei, L.; Kim, J.-H.; Wang, M.; Pootrakulchote, N.; Teuscher, J.; Di Censo, D.; Humphry-Baker, R.; Moser, J.-E.; Yu, Y.-J.; Kay, K.-Y.; Zakeeruddin, S. M.; Grätzel, M. *Energy Environ. Sci.* **2010**, *3* (7), 956.

(9) Hagfeldt, A.; Boschloo, G.; Sun, L.; Kloo, L.; Pettersson, H. *Chem. Rev.* **2010**, *110*, 6595 and references cited therein.

(10) Soler, J. M.; Artacho, E.; Gale, J. D.; Garcia, A.; Junquera, J.; Ordejon, P.; Sanchez-Portal, D. *J. Phys.: Condens. Matter* **2002**, *14*, 2745−2779.

(11) Frisch, M. J. et al. *Gaussian 09*; Gaussian Inc.: Wallingford, CT, 2009.

(12) Chai, J.-D.; Head-Gordon, M. *J. Chem. Phys.* **2008**, *128*, 084106.